Benha Journal of Applied Sciences (BJAS) print: ISSN 2356–9751
Vol. (8) Issue (5) (2023), (173-184) online: ISSN 2356–976x
http://bjas.journals.ekb.eg

The impact of rock-forming minerals on groundwater, Samalut aquifer, West Minia, Egypt

AL-SAYYAD M. A. [1], AGGOUR T. A. [1] ABU RISHA, U. A. [1], GRIESH M. H. [2], ARNOUS M. O. [2]

1 Geology Department, Water Resources and Desert Lands Division, Desert Research Center, Cairo, Egypt.
2 Geology Department, Faculty of Science, Suez Canal University, Ismailia, Egypt
Corresponding author: Mahmoudalsayyad@drc.gov.eg

ABSTRACT
The water-mineral interaction processes can strongly affect the quality of groundwater. The present study focuses on determining these processes and assessing their impact on the groundwater evolution in Samalut aquifer which is composed of fractured and karst carbonates. The aquifer was recharged mainly from Nile floods before the construction of Aswan High Dam (AHD). Forty-four groundwater samples of Samalut aquifer and three surface water samples of the Nile River, Ibrahimia Canal and Bahr Yusef Canal were collected and analyzed for major ions. The groundwater salinity ranges from 407 mg/l (well no. 33) to 2467 mg/l (well no. 17). It increases due northwest Six representative rock samples of Samalut Formation were collected from its outcrops and drilled wells. The mineral composition of these samples has been identified by X-Ray Diffraction (XRD). They are composed of calcite, dolomite, gypsum, anhydrite, halite, illite and ankerite. The mineral-water interaction processes were determined by the inverse hydrogeochemical modeling using NETPATH. These processes include the precipitation of calcite, the removal of calcium and magnesium in exchange for sodium as a result of freshening by the recharge from the Nile, and the dissolution of gypsum.

Keywords: West Minia, Mineralogy, groundwater evolution, NETPATH

INTRODUCTION

The study area is bounded by longitudes 29° 44' 9.60" E and 30° 56' 57.12" E and latitudes 27° 30' 1.43" N and 28° 35' 59.15" N (**Figure 1**). It is distinguished by good soil suitable for planting many essential crops depending on the groundwater resources. So, it is crucial to study the impact of mineral composition of the aquifer on the groundwater salinity to achieve agricultural development. The previous studies focused principally on the Nile Valley and its western desert fringes to the Western Desert Road (e.g., [1], [2], [3], [4], [5], [6] and [7]). The present study extends further to the west of this road.

The study area is arid with hot dry summer and warm winter with little precipitation, and high evaporation rates. The records of Minia meteorological Station between 1988 and 2006 [8] show that the minimum temperature varies from 1 °C in January to 18.1 °C in August, while the maximum temperature ranges from 25.1 °C to 44.3 °C between January and June. The region receives only 19.6 mm of precipitation annually on average during the rainy season, which lasts from the beginning of October to the end of May.

Based on [9] and [10], topographic maps (1:100000), digital elevation model (DEM-30 m), field observations, and previous literature, the study area can be geomorphologically divided into the Eocene Plateau, the Nile Valley, and the flood plain **(Figure 2 and Table 1).**

The Eocene plateau consists of carbonate rocks (mainly limestone) with clastic interbeds. Its surface comprises sandy plain, gravelly plain, isolated hills, sand dunes, playa sediments and drainage networks.

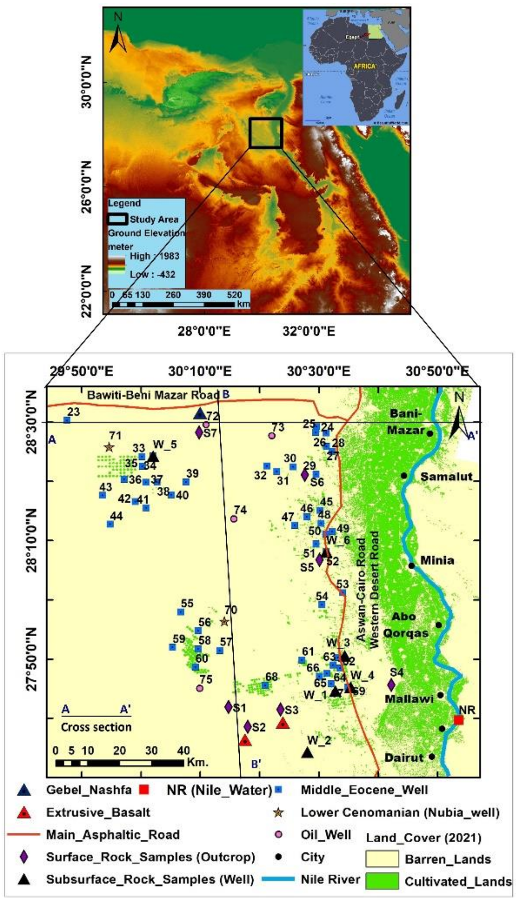

Figure 1: Location map of the study area

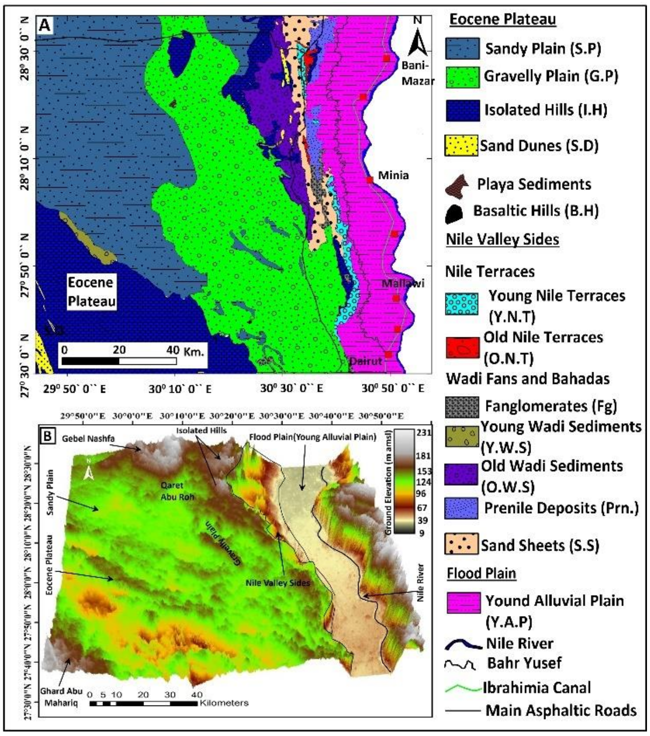

Figure 2: The main geomorphological units of the study area (A) and the 3D image (B) reflects the high and lowlands (m amsl)

The Nile Valley can be subdivided into Nile terraces, wadi fans and bahadas, and sand sheets. The flood plain width ranges from 13.4 km at Mallawi area to 23 km at Beni-Mazar showing that its width increases gradually from south to north. The flood plain is formed from recent Nile silt which has been deposited during the successive Nile floods that used to cover the plain before the construction of Aswan High Dam (AHD) (**Figure 2**).

The study of both surface and subsurface geological characteristics of this area helps understanding the hydrogeological setting and the evolutionary processes of groundwater salinity. The geological structures are composed of faults and fractures which are parallel either to the Gulf of Suez (NW-SE trend) or to the Gulf of Aqaba (NE-SW trend). These faults play a critical role in the groundwater occurrence [11], [1], [2] and [12]. The lithostratigraphic succession of the area was previously studied by many researchers e.g., [13], [14], [15] [16], [17], [18] and [19].

Based on the investigation of 185 logs, the thickness of clay increases due northwest. This clay is of small thickness or missed in the hanging walls of the effective faults. So, it affects the occurrence and quality of groundwater. Based on the geologic maps, field investigations including seven surface lithostratigraphic sections, subsurface samples of five drilled wells, 23 groundwater well logs, and reports of four oil wells in addition to the laboratory investigation of the lithofacies characteristic, the stratigraphic successions of both the surface and subsurface rock units were defined. The study area is covered by rocks ranging in age from Lower Eocene to Recent (**Figure3 and Figure 4**). A special attention was paid to Samalut Formation as it represents the main aquifer in the area.

Table 1: Parameters of geomorphological units of the study area

Geomorphologic features		Area (km^2)	Perimeter (km)	Elevations (m.a.s.l)	
Unit name	Subdivisions			From	To
Eocene Plateau	Sandy plain	3481	542.4	105	189
	Gravelly plain	3920	367.2	105	164
	Isolated hills	99.1	76.6	90.5	205
	Sand dunes	55.7	134.3	76	194
	Playa sediments	3.7	9.3	103	108
Nile Valley Sides	Young Nile Terraces	157	170.04	37	116
	Old Nile Terraces	65.2	86	50	106
	Fanglomerates	89.5	134.8	38.5	147
	Young Wadi Deposits	74	68.2	71.6	142
	Old Wadi Deposits	497	187.3	81.9	125
	Prenile Deposits	175	134.6	34.6	66
	Sand sheets	329	311.8	37.7	162
Flood plain		2099	307.3	16	50

Samalut Formation (SF) was deposited under reefal conditions (shallow marine limestone) with Nummulites gizehensis and Globigerinoids reflecting middle Eocene age [20]. It consists of white and chalky limestones with some marl and claystone interbeds at the eastern part of the study area. It laterally changes to dolomitic limestone and dolostone close to Qaret El-Soda (**Figure3**). It is characterized by the presence of clay bed which represents the cap or confining bed of Samalut aquifer, bands of coal, paleokarst features, shaft sand cave. Its total thickness ranges from 215 m at Qaret El-soda (Well no 75) to about 1091 m at Qaret Abu Roh (well no 73). Based on the investigation of 185 logs, the thickness of clay increases due northwest.

This clay is of small thickness or missed in the hanging walls of the effective faults. So, it affects the occurrence and quality of groundwater. Based on the logs of four oil wells tapping basement rocks (well nos. 72, 73, 74 and 75) and deep water well no. 70 tapping the Lower Cenomanian Bahariya Formation. The subsurface rocks range in age from Pre-Cambrian to Oligocene (**Figure 4**). The subsurface Eocene rocks were named Apollonia Formation by the oil geologists [21]. In the study area, the thickness of these rocks' ranges between 154 m (well no. 72) at the north and 1227 m (well no. 73) at the northeast of the study area.

Structurally, the study area is affected by various structures including joints, faults, and folds [13], [9] and [10]. In the recent study, the structural lineaments density and frequency are the greatest in the areas A5, D2, E3, F3, F6, G3, and G4, where they are close to the fault planes and the extrusive volcanics which are recorded at Qaret El-Soda at the south of the study area (**Figure 5A**).

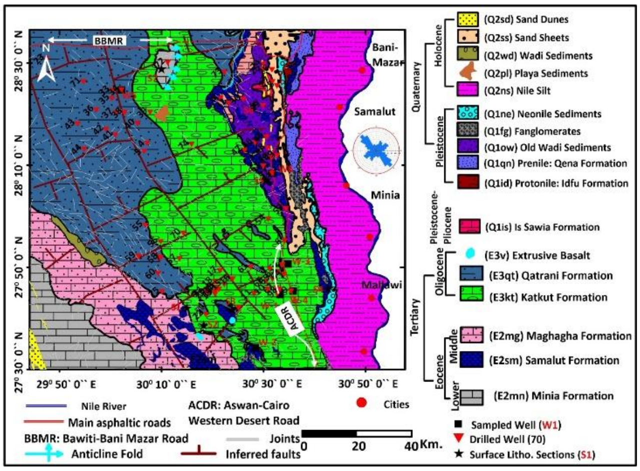

Figure3 : Geological map of the study area modified after (Conoco, 1987, EGSMA, 2005 and Saada S. A. and El-Khadragy A. A. ,2015)

These areas represent the best places for natural recharge when flash floods occur. Moreover, the rose diagram indicates two main sets of lineaments which are directed NW-SE (Gulf of Suez direction) and NE-SW (Gulf of Aqaba direction).

The subsurface structures of the study area were studied by many authors among them [13], [22], and [23]. The study area was affected by three sets of faults; NE-SW, NNE-SSW and NNW-SSE **(Figure 5B and Figure 6).** These faults created a series of horsts and grabens and in turn the thickness of Samalut aquifer is greater in the graben than in the horst. A monocline was recorded at the Gebel Nashfa where the fold influenced by a normal fault Consequently, the older stratum represented by Minya Formation (Lower Eocene) has recorded at the core of Gebel Nashfa and is surrounded by younger strata (Middle Eocene and Oligocene).

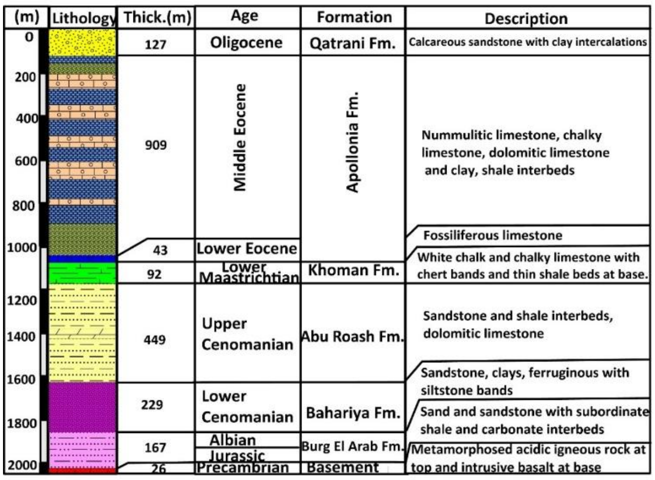

Figure 4: Recorded subsurface rock units of the study area at the north of the study area (well no. 74).

MATERIALS AND METHODS

The rock samples were analyzed by using X-ray powder diffraction (XRD) to determine the mineral composition. On the other hand, 44 water samples of Samalut aquifer were collected in 2021. The depth to groundwater was measured to create the flow map of the investigated area. The X-ray diffraction (XRD) analytical techniques were used to identify the aquifer rock-forming minerals of 6 samples collected from recently drilled wells and outcrops scattered over the area representing the water carrying formation of the study area. XRD analysis was carried out in the central laboratories of the Egyptian Mineral Resources Authority, (previous, Egyptian Geological Survey).

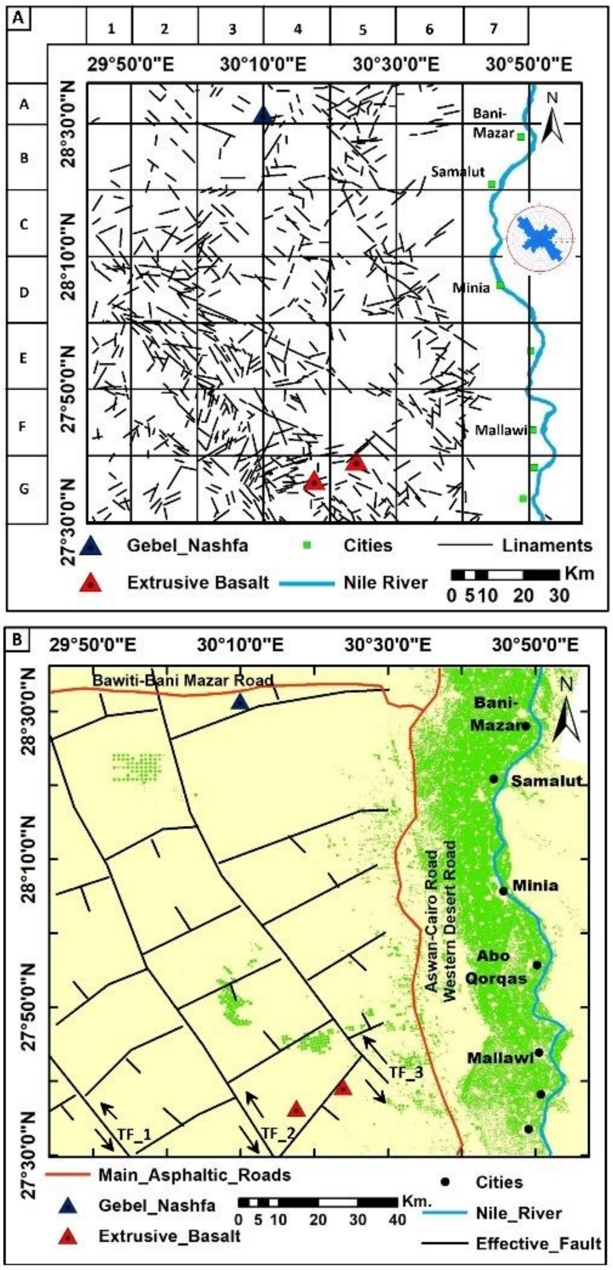

Figure 5: Structural lineaments map of the study area which extracted from (CONOCO, 1987) and the rose diagram(A); the effective faults (B) modified after Saada S. A. and El-Khadragy A. A. (2015); TF1, TF2 and TF3 are confirmed faults by cross sections.

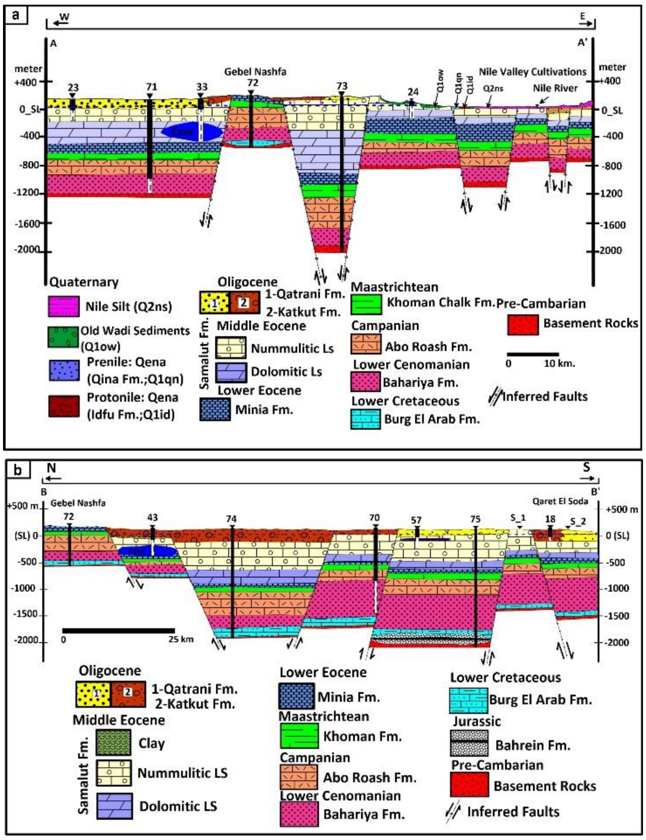

Figure 6: AA` Geologic cross section in the study area from West to East (modified after EGSMA, 2005) and BB` geologic cross section from North to South along the study area.

For water samples, each well was pumped for about ten minutes at least until the temperature and electrical conductivity (EC) stabilized. During this study, 44 groundwater samples from the Middle Eocene aquifer and one sample from Nile River, were collected. The pH and EC were measured on-site by Jenway, 3150 and Jenway, 470 portable meters.

These samples were chemically analyzed by using ICP Spectrometer for major ions (Ca^{2+}, Mg^{2+}, Na^{+}, K^{+}, SO_4^{2-} and Cl^{-}) while the carbonate anions (HCO_3^{-} and CO_3^{2-}) were measured by titration with 0.05 N HCl and Phenolphthalein and methyl orange as the indicator at the hydrochemistry laboratory of the Desert Research Center.

According to the methods adopted by U. S. Geological Survey [24], the ionic charge balance of these analyses was within ± 5 %. Finally, the depth to groundwater was measured by using Solinst Water Level Meter model 102 to create the flow map of the investigated area. The inverse hydrogeochemical modelling code NETPATH [25] was used to analyze how groundwater changed along the flow path.

RESULTS AND DISCUSSION:

Mineralogically, the obtained X-ray diffractograms (Figure 7) are interpreted according to the diagnostic diffraction maxima of each mineral established by [26], [27], [28] and based on ASTM data and the methods described by [29]. The studied samples of the Samalut Formation reveal the presence of various minerals which will be interpreted. The references of the used cards for identification of the measured minerals and the semi quantitatively percentage of each mineral are shown in Table 2. The Samalut Formation is characterized by the existence of calcite, dolomite and ankerite as dominant minerals followed by gypsum, anhydrite, and halite, and at the end illite mineral. Most samples contain calcite and dolomite, and it becomes argillaceous and ferruginous to the south of Qaret El Soda due to the presence of illite and ankerite as in the surface lithostratigraphic section S3. On the other hand, gypsum, anhydrite, and halite exist at the eastern scarp of the Eocene Plateau (section S5, Figure 7).

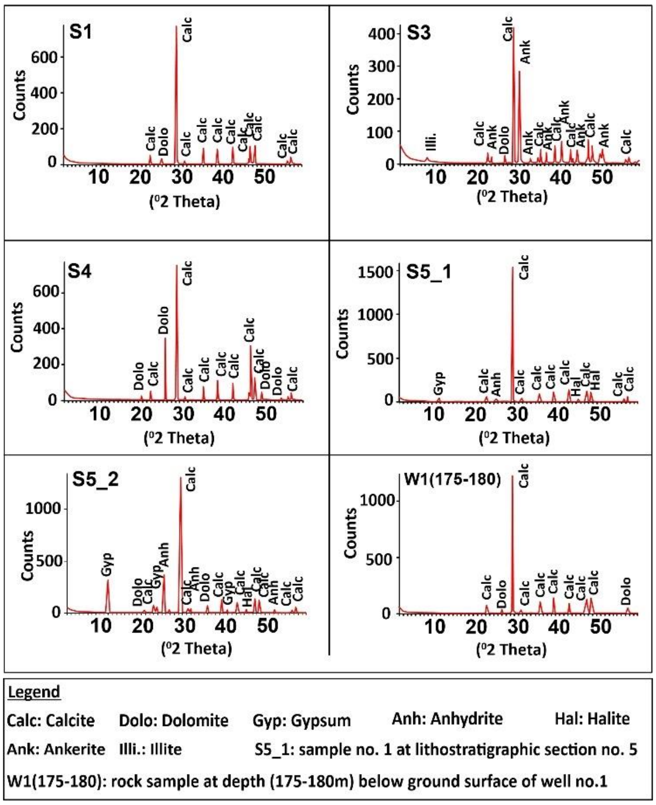

Figure 7: X-Ray Diffractograms of bulk samples of Samalut

Samalut aquifer is a fractured limestone water-bearing formation. The level of the upper surface of the water-bearing fractured limestone attains 171 m a.s.l (well no. 73) at the north, and 122 m a.s.l (well no. 75) at the south. On the other hand, at the middle part of the study area, this level ranges from -139.38 m b.s.l (well no. 40) at the northwest of the study area to -134.1 m b.s.l (well no. 71) (Figure 8A). The depth to water from the drilled wells tapping this aquifer ranges from 46 m (well no. 26) to 133 m (well no. 32) (Figure 9A)

The total depth ranges between 165 m (well no. 69) at the southeastern part of the study area to about 650 m (well no. 71) at the northwestern part (Table 3). Hence, the measured saturated thickness of this aquifer increases gradually from southeast recording 78.8 m to northwest recording 273 m. Its electric conductivity of the groundwater ranges from 770 µMoh/s (water sample no. 33) to 4300 µMoh/s (water sample no. 17) **(Figure 9B).**

The water level is mainly structurally controlled where the northern and southern parts represent hanging walls of graben faults, whereas the middle part is the foot wall of these faults. These graben faults are confirmed by the BB` cross section (**Figure 6**) and the top level of Samalut Formation map (**Figure 8**). Additionally, the thickness of clay (confining bed of Samalut aquifer) increases from southeast to northwest of the study area.

Therefore, the water level is higher in the northwest as the penetration of confining bed create artesian conditions. As well as the return of excess irrigation water and the breakage of the concrete tanks (common in the study area) participate in increasing water level. On the other hand, because of over pumping for irrigation, the local groundwater flow patterns have been established (low water levels). In conclusion, the groundwater flow direction was directed from southeast to northwest before the construction of High Dam, whereas this flow direction was reversed after the construction of this dam.

The hosted water in the Middle Eocene fractured limestone aquifer was formed as a result of the recharge of Nile water before the construction of High Dam. Samalut aquifer is expected to receive variable recharge from rainfall as well as the potential for upwelling from the Nubian Sandstone Aquifer (NSA) into the Eocene aquifer [30]., in addition to the return of extra irrigation water.

Inverse hydrogeochemical modeling

To interpret the water-rock interaction, significant ion chemistry of groundwater and aquifer materials were combined because the hydrogeochemistry of groundwater is unable to fully describe the geochemical evolution on its own [31]. In addition, several researchers have created and characterized geochemical models that, assuming equilibrium, describe solution/precipitation and other chemical processes [32], [33].

This section's major goal is to pinpoint the geochemical mechanisms in charge of regulating groundwater composition. As a result, along the flow path, geochemical reaction models for the entire groundwater system were created. The investigation of mineral phases and the chemical makeup of the groundwater served as limitations for the models. This will help to explain the water-rock interaction in the research area.

In general, the groundwater evolves chemically along the flow path and vadose zone due to the interaction between rainwater and various rock forming minerals. Dissolution predominates in the recharge-through area, ion exchange in the flow area, while evaporation, precipitation and ion exchange predominate in the discharge area with the change in major ions from HCO_3^- and Ca^{2+} to Cl^- and Na^+ [34], [35] and [36].

Table 2: The investigated mineral composition of Samalut Formation

S.N.	Ref. Code	Mineral Name	Chemical Formula	Semi Quant [%]
S1	01-072-4582	Calcite	$CaCO_3$	97
	01-075-3699	Dolomite	$CaMg(CO_3)_2$	3
S3	01-085-0849	Calcite	$CaCO_3$	60
	01-074-7798	Ankerite	$CaMgO_{.67}FeO_{.33})(CO3)_2$	35
	01-075-3699	Dolomite	$Ca\,Mg(CO_3)_2$	3
	00-058-2015	Illite	$(K,H_{30})\,Al_2(\,Si_3\,Al\,)\,O_{10}\,(\,O\,H\,)_2$ x H2O	2
S4	01-076-2712	Calcite	$CaCO_3$	70
	01-075-3699	Dolomite	$CaMg(CO_3)_2$	30
S5_1	01-076-2712	Calcite	$CaCO_3$	90
	01-070-2509	Halite	NaCl	2
	01-072-0916	Anhydrite	$CaSO_4$	4
	00-036-0432	Gypsum	$CaSO_4.2\,H_2O$	4
S5_2	01-083-0578	Calcite	$CaCO_3$	60
	01-071-4661	Halite	NaCl	3
	01-075-3699	Dolomite	$CaMg(CO_3)_2$	5
	00-006-0046	Gypsum	$CaSO_4.2\,H_2O$	20
	01-086-2270	Anhydrite	$CaSO_4$	12
W1(175-180)	01-083-0578	Calcite	$CaCO_3$	97
	01-075-3699	Dolomite	$CaMg(CO_3)_2$	3

As a result, chemical evolution of groundwater can be inferred because the change in groundwater composition is resulted from the effect of these processes. Wells were chosen along the flow path to examine the geochemical evolution within the study area (**Figure 9A**). West Minia has both regional and local flow system that is influenced by structure, and agricultural activities. A list of the wells sampled for the study is given in **Figure 9B**.

Table 3: Hydrogeological data of the Middle Eocene limestone aquifer

Well no.	Total Depth (m)	Ground Elevation (m a.m.s.l)	Depth to water (m)	Water level (m.a.s.l)
23		145	107	42
24		87	58.5	38.5
25		87	54.18	32.82
26		87	46	41
27		86	48.39	37.61
28		81	46.23	34.77
29		87	52.9	34.1
30		129	90.1	38.9
31		130	92.12	37.88
32		173	133.05	39.95
33	650	125.9	89.3	36.6
34	370	152	111.16	40.84
36	450	116.85	81.52	35.33
38		136	92	44
39	500	138.86	90.4	48.46
40	600	135.62	99.62	36
42	500	109.11	70.95	38.16
43	600	117	80.33	36.67
44	550	117	78.9	38.1
45		93	57.98	35.02
46		102	72	30
47		146	111.45	34.55
48		107	71.38	35.62
51		149	112.5	36.5
52		119	85.43	33.57
54	227	138	64	74
56	399	125	89	36
57	351.5	120	87.1	32.9
58	360	103	67.3	35.7
59	390	124	83.5	40.5
60	353	124	87.6	36.4
62		126	93.16	32.84
64	240	132	150	-18
65	229	122	83.4	38.6
66	224	126.79	86.5	40.29
67	260	128	120	8
68	175	125	90	35
69	165	130	86.2	43.8

On the other hand, the analysis of rock samples from the water bearing formation, Samalut aquifer, is intended to show the distribution of the different rock forming minerals and their effects on groundwater composition. Based on mineralogy and calculated saturation indices (**Table 5**), the possible mineral phases were selected for the modeling of the geochemical evolution of the groundwater system

These mineral phases react with the groundwater and act as sources for the changing composition of the groundwater along the flow path. These mineral phases react with the groundwater and act as sources for the changing composition of the groundwater along the flow path.

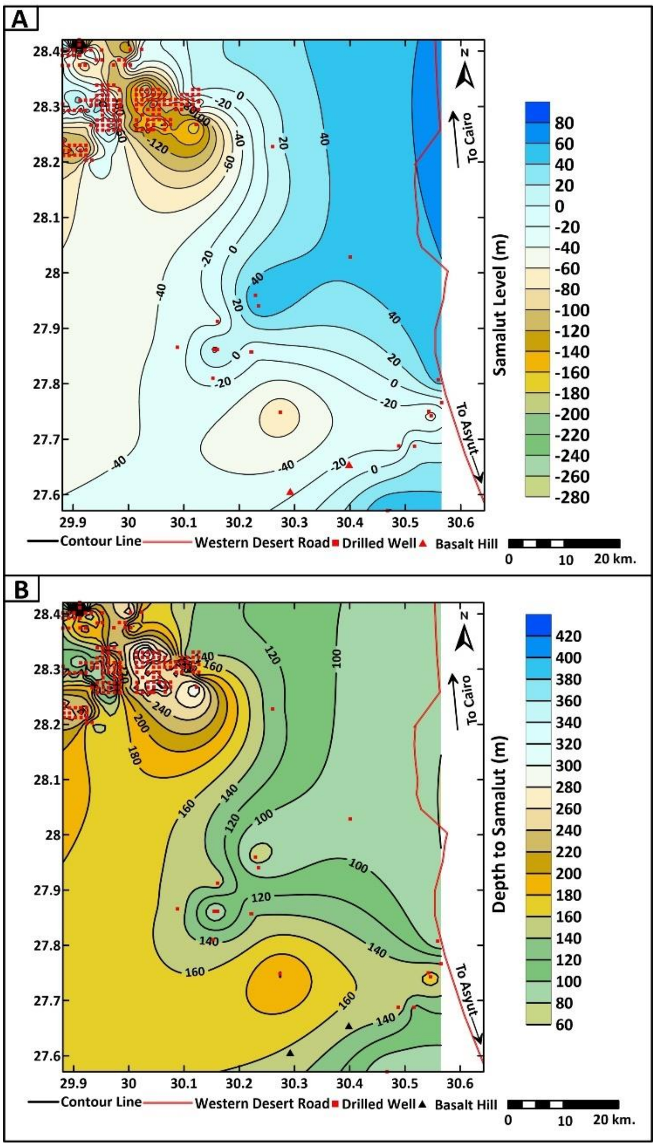

Figure 8: Top level map of Samalut Formation m. a s. l(A) and depth to Samalut Formation from ground surface (B).

Calcite is thermodynamically preferred to dissolve and contribute calcium and bicarbonate ions into the groundwater system. The presence of clays indicates the potential for cation exchange process.

A distinct hydrogeochemical process was considered in determining the chemical evolution of the groundwater salinity which is reactions of groundwater as it moves from a high head groundwater area (recharge area, Nile River before the construction of High Dam) down gradient to a low head of groundwater area (discharge area, northwest of the study area, the same direction of buried channels) (**Figure 9A**).

The NETPATH model results provided as many models as possible based on different constraints and phases used (**Table 6**). In each case, numerous runs were made, and less realistic models were excluded, with realistic model results repeating the groundwater conditions under consideration. Negative values indicate precipitation and positive indicate dissolution (**Figure 10**).

Table 4: The saturation indices of the groundwater with respect to different minerals

No. Phase	Nile River	Sample no. 9
Calcite	-0.260	-1.208
Aragonite	-0.409	-1.348
Dolomite	-0.633	-1.999
Gypsum	-2.306	-1.214
Anhydrite	-2.552	-1.409

The inverse geochemical model explains that the saturation indices of the Nile water (initial point) are negative values demonstrating the dissolution of both carbonates and evaporites. Additionally, the saturation indices at well no. 9 (final point) are all negative values of calcite, aragonite, dolomite, gypsum, and anhydrite reflecting sub-saturation and potential for dissolution of these minerals.

According to the results of the geochemical modeling (**Table 7**), the negative values interpret the precipitation of calcite causing the removing of $Ca^{2+}$and HCO_3^- ions from solution, while the positive value of gypsum indicating the dissolution of it adding the Ca^{2+} and SO_4^{2-} ions to the water. The positive value of ion exchange reflects the high content of Na^+ ion with a subsequent formation of illite and other clay minerals. Finally, the positive value of Mg/Na exchange indicates the adding of Na^+ ions and removing of Mg^{2+} ions into/from well no. 9. (**Table 7**). Also, the results indicate that the solutes contained in 1 kg of water from well no. 9 would be concentrated by factor 4.586 leaving only 218.044 gm H_2O remaining.

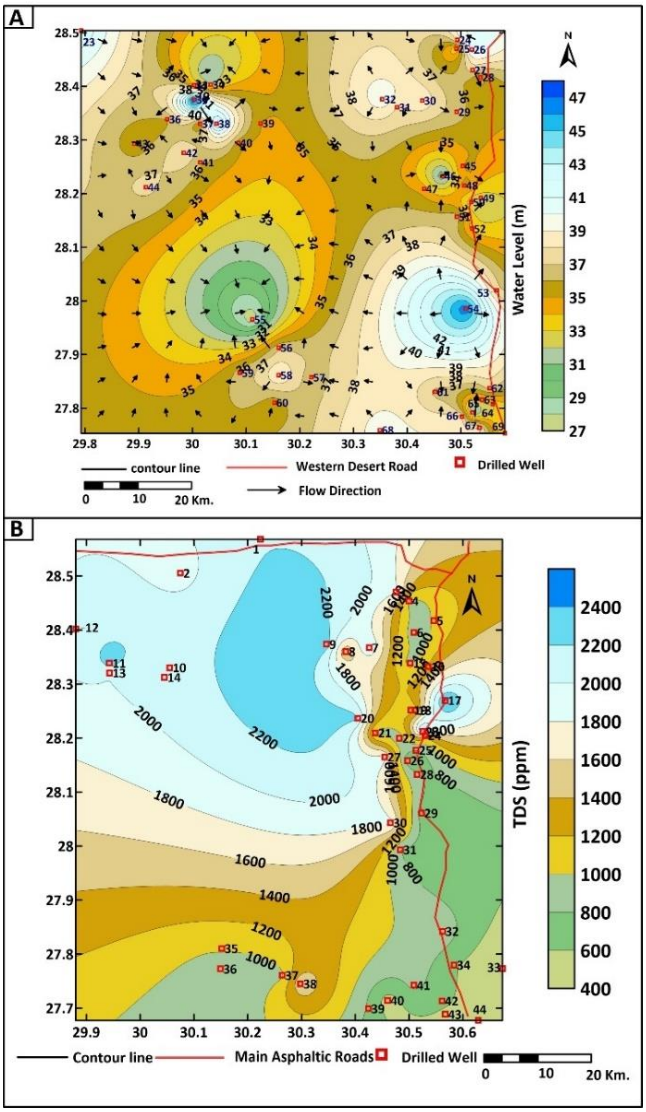

Figure 9: Recent Water level map (A) and iso- salinity map (B) of Samalut aquifer

Table 5: Concentrations of major ions (ppm) in the studied samples

Well No.	Ca^{++}	Mg^{++}	Na^{+}	K^{+}	CO_3^{--}	HCO_3^{-}	SO_4^{--}	Cl^{-}	TDS	pH	T° C
*NR	45	20	8	5	0	158.6	34	425	236.3	7.5	16.8
1	261	76	400	26	24	195.2	270	275	2179.60	8.2	27.7
2	224	75	350	24	0	219.6	165	350	1922.80	8	26.1
3	41.6	121.3	460	12.4	0	111	279.1	875	1844.92	7.11	19.8
4	149.8	20.2	140	8.5	0	87.24	229.43	340	931.53	7.36	24.6
5	58.24	75.8	190	8	0	55.51	301.21	375	1036.02	7.22	27
6	41.6	60.7	180	7.8	0	47.51	188.24	380	882.04	8.22	25.4
7	124.8	111.2	420	13.2	0	103.1	502.42	800	2023.16	7.06	28.5
8	91.52	45.5	370	10.7	0	47.58	-61.53	900	1379.97	7.76	23.5
9	91.52	96	600	18.6	0	23.79	471.16	1050	2339.21	7.1	30.5
10	124.8	80.9	520	22.7	0	39.65	319.48	1025	2112.67	7.96	30.5
11	116.5	80.9	580	22.2	0	63.44	483.9	975	2290.18	7.11	33.3
12	160	70	480	27	60	244	145.89	325	2039.89	7.8	29.8
13	141.4	85.9	440	21.3	0	71.37	314.19	975	2013.54	7.06	
14	133.1	80.9	500	21.8	0	39.65	368.04	975	2098.65	7.91	31.5
15	87.36	17.7	220	8	0	47.54	105.23	460	922.05	8.2	26.5
16	99.84	65.7	230	8.4	0	71.37	425.73	375	1240.37	6.6	26
17	380	72	365	15	12	366	530	280	2467.00	7.8	23.2
18	58.24	85.9	200	7.1	0	47.58	367.08	375	1117.13	7.28	26.6
*19	124.8	80.9	2450	23.5	0	63.44	794.22	4900	6816.7	6.7	24.9
20	99.84	91	580	13.3	0	95.16	386.31	1025	2243.01	7.97	28.9
21	83.2	50.5	160	7.8	0	71.37	231.74	350	918.97	6.94	26.5
22	83.2	55.6	150	7.1	15.6	63.44	132.25	400	875.47	7.78	28.6
23	124.8	85.9	620	11.4	0	79.3	417.32	1100	2399.10	6.46	27.4
24	92	43	280	7	18	231.8	200	160	1205.90	7.8	26.5
25	58.24	40.4	160	6.5	0	96.16	218.98	260	792.24	7.27	25
26	66.56	40.4	110	5.9	0	95.16	118.53	275	664.00	6.78	27.1
27	83.2	85.9	480	11.2	0	79.3	370.68	830	1900.65	7.22	28.9
28	74.88	55.6	135	6.3	0	63.44	166.84	350	820.34	7.85	27
29	98.07	44.4	85	6	12	170.8	85	350	685.87	8.2	25.6
30	149.8	40.4	390	8.5	0	39.65	956.74	300	1865.26	6.59	25.5
31	76.45	35.56	165	7	12	256.2	138.03	337.5	802.14	8.2	24.4
32	103.8	35.78	180	18	24	134.2	94	300	932.68	8.2	25.4
33	57.73	23.06	56	5	24	183	70	387.5	407.29	7.9	21
34	72.16	27.86	115	6	24	195.2	43.94	275	616.56	8	23.6
35	94	58	195	9	36	183	140	325	1033.50	7.3	25
36	83.2	40.4	160	8.9	0	39.65	177.7	370	860.06	8.15	24.5
37	115	55	130	9	48	183	325	400	943.50	7.4	27.7
38	140	75	330	9	18	231.8	184.7	195	1572.60	7.2	27.5
39	83	55	120	7	12	207.4	105	150	775.70	7.4	26.6
40	61	30	84	6	24	170.8	45	275	505.40	7.4	24.4
41	110	60	110	9	48	122	64	300	849.50	7.3	22.9
42	72.99	26.15	135	7	36	231.8	78	450	661.04	7.6	24.7
43	51.78	24.08	110	7	36	183	130	250	550.36	7.4	22
44	59.83	25.51	88	6	24	256.2	88	80	499.44	7.4	25.7

*NR: Nile River *19: is a mixed water (non-representative)

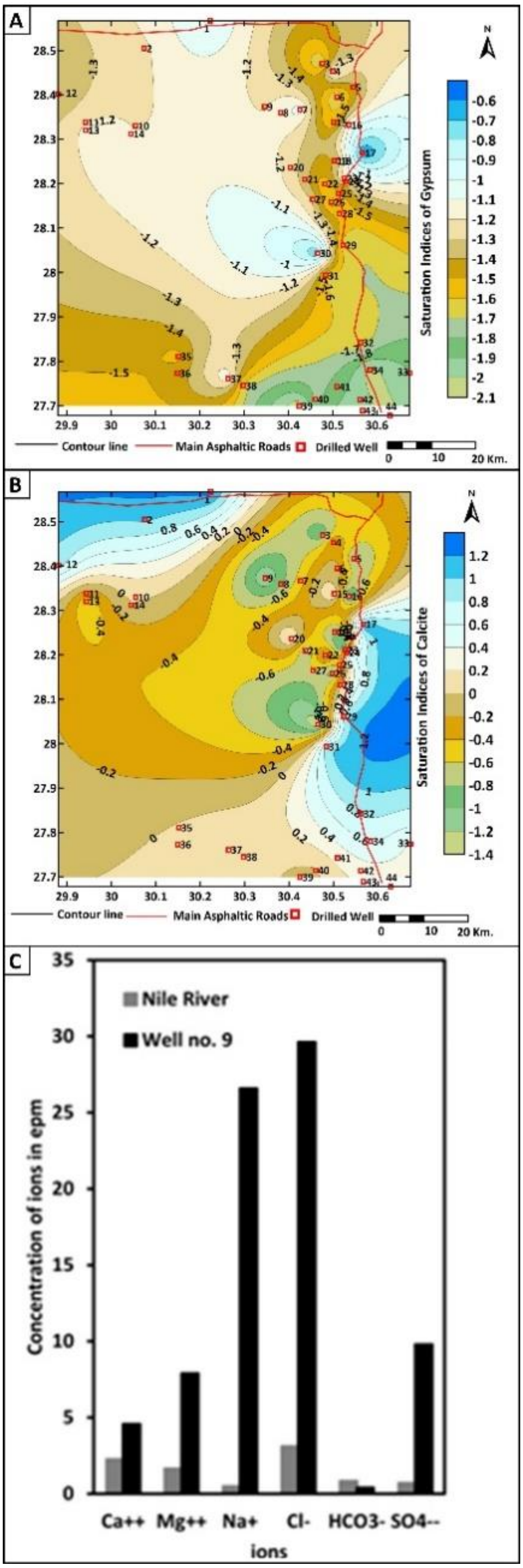

Figure 10: Areal distribution of the gypsum saturation indices (A), calcite saturation indices (B) of the studied groundwater of Samalut aquifer and the evolution of groundwater along the flow path (C)

Table 6: The constraints and phases used for geochemical modeling

Constraints	Phases
Sulfur	Gypsum
Calcium	Calcite
Magnesium	Exchange
Sodium	Mg/Na Exchange
Chloride	

Table 7: Results of geochemical modelling

well list		phase	Composition	Delta	Evap. Factor	Remain in (g H2O)
initial	final					
Nile River	Well no. 9	Calcite	$CaCO_3$	-0.59	4.586	218.00
		Gypsum	$CaSO_4.2H_2O$	1.89		
		Exchange	Ca /Na	0.87		
		Mg/Na EX	Mg/Na	0.66		

CONCLUSIONS:

In conclusion, the Samalut aquifer's mineral composition directly affects the salinity of the groundwater. The Samalut aquifer is discovered to be more gypseous near the eastern scarp of the Eocene Plateau, where it is more argillaceous and ferruginous, according to the results of the bulk X-Ray diffraction research. In addition, the primary sources of various ions in groundwater include calcite and gypsum minerals, as well as ion exchange. Along the flow path, the groundwater changed from a weak Ca-Cl solution (Nile water) to a strong Na-Cl solution (well number 9). The major chemical species from these sources are Na^+, Ca^{2+}, Mg^{2+} $HCO_3^-$and SO_4^{2-}

REFERENCES

[1] Shabana, A. R. (2010): Hydrogeological Studies on the Area West Deir Mouas-Mallawi, El Minia Governorate, Egypt. Egyptian Journal of Geology, 54, 61-78.

[2] El Kashouty, M., Aziz, A. A., Soliman, M., and Mesbah, H. (2011): Hydrogeophysical investigation of groundwater potential in the El Bawiti, Northern Bahariya Oasis, Western Desert, Egypt. Arabian Journal of Geosciences, 5(5), 953-970.

[3] Al Temamy, A. M. and Abu Risha, U A. (2016): Groundwater interaction and potential: inferred from geoelectrical and hydrogeological techniques in The Desert fringe of Abu Qurqas area, El Menia, West Nile, Egypt, Egyptian Journal of Geology, v. 60, p. 75-95.

[4] Salem, A. A. (2016): Hydrogeological studies on the shallow aquifers in the area west Samalot, El-Minia Governorate, Egypt. Egy. J. Pure and Appl. Sci. 2015; 53(4): p 49-60.

[5] Ibrahim, R. G., & Lyons, W. B. (2017). Assessment of the hydrogeochemical processes affecting groundwater quality in the Eocene limestone aquifer at the desert fringes of El Minia Governorate, Egypt. Aquatic Geochemistry, 23, 33-52.

[6] Mousa, A. A. (2018): Geology of Groundwater Resources in The Western Desert fringes of El Minia Governorate, Egypt (M Sc. Thesis, Al-Azhar University).

[7] Ibrahem, S., Elalfy, M., andHagras, M. (2020): Groundwater potentials of Eocene limestone aquifer in West-West El-Minya area, Egypt. Egyptian Journal of Desert Research, 70(1), 59-82.

[8] Egyptian Meteorological Authority, (2014): Meteorological data of different stations in west El-Minia.

[9] Egypt, C. C. (1987): Geologic map of Egypt (Scale 1: 500000). General Petroleum Company, Cairo, Egypt.

[10] EGSMA, Egyptian Geological Survey and Mineral Authority, (2005): Geologic Maps of Minia. Scale 1:250,000 Sheet 2. Geol. Surv. Egypt, Cairo, Egypt.

[11] Youssef M. I. (1968): Structural pattern of Egypt and its interpretation. Bull. Amer. Petrol. Geol., V. 52. No. 4, pp. 601-614.

[12] Embabi, N. S. (2018): Landscapes and landforms of Egypt. Springer.

[13] Said, R. (1962): The Geology of Egypt. El Sevier, 377 p.

[14] **Khalifa M. A. (1981):** Geological and sedimentological studies of west Bani Mazar area, south El-Fayum province, Western Desert, Egypt. Ph.D. Thesis.

[15] **Mansour, H. H. and Philobbos, E. R. (1983):** Lithostratigraphic classification of the surface Eocene Carbonates of Nile Vally, Egypt. Areview. Bull. Fac. Sci, Assuit Univ., 12(2c).

[16] Abdel Aziz, R. S. (1994): Geological and sedimentological studies In West El Minia - Bani Mazar area, Egypt. M.Sc. Thesis

[17] Issawi, B., El-Hinnawi, M., Francis, M., and Mazhar, A. (1999): The Phanerozoic geology of Egypt Ageodynamic approach Special Publication No. 76. Geol. Survey Cairo.

[18] Zaki, R. (2007): Pleistocene evolution of the Nile Valley in northern Upper Egypt. Quaternary Science Reviews, 26(22-24), 2883-2896.

[19] Abdel Baky, N. F. (2013): Exploring groundwater possibility in the area west of El Fayoum-Asuit road using remote sensing, geophysical and GIS techniques. Ph.D. Thesis. Fac.Sci., Cairo University, pp. 168.

[20] Boukhary, M. and W. Abdelmalik, (1983): Revision of the stratigraphy of the Eocene deposits of Egypt. N.Jb. Geol.Palaeont., Mh., 6. P. 321-337.

[22] El-Kenawy AA (2000): Interpretation of potential field data of the area between latitudes 27̊ 30′ -29̊ 00′N and longitudes 26̊ 00′E, Western Desert, Egypt. Ph. D. Thesis Fac Sci Zagazig Univ.

[23] Saada, S. A., and El-Khadragy, A. A. (2015): An Integrated Study of Gravity and Magnetic Data on West El-Minya Area, Western Desert, Egypt. Journal of American Science, 11(12), 169-184.

[24] ASTM, American Society for Testing Materials (2002) in: Water and environmental technology, Annual book of ASTM standards, 11, (11.01 and 11.02), West Conshohocken, U.S.A.

[25] Plummer, L. N., Prestemon, E. C., and Parkhurst, D. L. (1994): An interactive code (NETPATH) for modeling net geochemical reactions along a flow path, US Geological Survey Reston, VA.

[26] Black, C. A. (1965): Methods of Soil Analysis Part 1 And 2, American Society of Agronomy, Inc.; USA.

[27] Carver, R. E. (1971): Procedures in sedimentary petrology, John Wiley and Sons Incorporated.

[28] Brown, G. 1972. The X-ray identification and crystal structures of clay minerals.

[29] Millot, G. (1970): Geology of Clays Chapman and Hall. London (Engl. transl. WR Farrand and H. Paquet).

[30] Korany, E. A., Tempel, R. N., Gomaa, M. A., & Mohamed, R. G. (2013). Detecting the roles of the physiochemical processes on groundwater evolution, Assiut area, Egypt-applications of hydrogeochemical and isotopic approaches. *Egypt J Geol*, *57*(2013), 63-83.

[31] Locsey, K. L., Grigorescu, M. and Cox, M. E. (2012): Water–rock interactions: an investigation of the relationships between mineralogy and groundwater composition and flow in a subtropical basalt aquifer. Aquatic geochemistry, 18, 45-75.

[32] El Kadi, A. I., Plummer, L. N., and Aggarwal, P. (2011): NETPATH-WIN: An interactive user version of the mass-balance model, NETPATH. Groundwater, 49, 593-599.

[33] Parkhurst, Dl and Appelo, C (2013): Description of input and examples for PHREEQC version 3: a computer program for speciation, batch-reaction, one-dimensional transport, and inverse geochemical calculations, US Geological Survey, USA.

[34] Tóth, J. (1999): Groundwater as a geologic agent: an overview of the causes, processes, and manifestations. Hydrogeology journal, 7, 1-14.

[35] Adams, S., Titus, R., Piersen, K., Tredoux, G., and Harris, C. (2001): Hydrochemical characteristics of aquifers near Sutherland in the Western Karoo, South Africa. Journal of Hydrology, 241, 91-103.

[36] Wang, L., Li, G., Dong, Y., Han, D., and Zhang J., 2015. Using hydrochemical and isotopic data to determine sources of recharge and groundwater evolution in an arid region: a case study in the upper–middle reaches of the Shule River basin, northwestern China. Environmental Earth Sciences, 73, 1901-1915.